LIGHT SCATTERING FROM NUCLEATED BIOLOGICAL CELLS

RICHARD A. MEYER *and* ALBERT BRUNSTING

From the Johns Hopkins Applied Physics Laboratory, Silver Spring, Maryland 20910, and the Physics Department, Auburn University, Auburn, Alabama 36830.
Dr. Brunsting's present address is Coulter Electronics, Inc., Hialeah, Florida 33010.

ABSTRACT The light scattered from nucleated biological cells has been investigated by using four different theoretical models: an opaque disk, a homogeneous sphere, an opaque ring, and a coated sphere. By comparing these four models, diffraction at the edges of the cell and the nucleus has been found to be the predominate scattering mechanism for nucleated biological cells at low angles. The scattering patterns of nucleated cells are found to have a fine lobe (high-frequency) structure dependent on whole cell size, and an envelope lobe (low-frequency) structure dependent on relative nucleus size. The models indicate that the present technique for measuring cell size with a single low-angle light detector is highly dependent on the nucleus to cell diameter ratio. Whole cell size is better estimated by the ratio of the outputs from two low-angle detectors.

INTRODUCTION

When a biological cell is illuminated with laser light, the light is scattered in all directions (i.e., deflected from the incident direction) (1). This light scattering is due to a number of different phenomena including: (*a*) diffraction of the light at the edges of the cell, the nucleus, and other cellular inclusions; (*b*) refraction (i.e., phase shifting and bending of the rays) due to the different relative index of refraction for the nucleus, cytoplasm, and surrounding medium, (*c*) reflection at the different optical boundaries within and enclosing the cell; and (*d*) absorption within the cell. Therefore, the scattering pattern is dependent on the morphology of the cells.

In this paper, we have used four different theoretical models to approximate the scattered light from biological cells and have examined the effect of changes in whole cell size and nucleus size on the scattering pattern. The eventual goal of this work is to recognize the light scattering patterns of various classes of cells in automated instrumentation. Our immediate goal here is to indicate the important physical processes of light scattering from nucleated cells and to suggest how these processes can be used for extracting the morphological information from these cells.

In this analysis, the nucleus and cytoplasm are assumed to be homogeneous and isotropic. The optical effects of the nonsymmetrical positions of cellular organelles are, therefore, ignored. However, intracellular heterogeneities can be thought of as contributing to the effective refractive indices of the cytoplasm and nucleus.

Light Scattering Models

In this section, the four different theoretical models used in this study are described, and some of the results published by others using these models are briefly reviewed. A very simple light scattering model for a biological cell is the two-dimensional, opaque, circular disk (2). Here the normal to the plane of the disk is parallel to the direction of the incident light. All the light intercepted by the disk is absorbed, while the light passing near the disk's edge is diffracted. The effects of cellular and nuclear reflection, refraction, and absorption are ignored. Since the only cellular parameter is the radius of the disk, the scattered light described by this model responds only to cell radius.

The light scattering pattern from a circular disk is well known and described by the Airy ring pattern (3). The angular width of the forward scattering lobe is inversely proportional to the radius, r_2, of the disk and directly proportional to the wavelength, λ, of the incident light. Since this model explains forward light scattering from cells satisfactorily (2), a measurement of the width of this central lobe results in information related to the diameter of the cell.

A homogeneous sphere model can be used to account for diffraction at the edge of the cell, as well as reflection and refraction at the surface of the cell. This three-dimensional model includes the additional cell parameter of mean refractive index. It has been shown that the scattering pattern of a homogeneous sphere is very similar in structure to the diffraction pattern of an opaque disk (4,5). The central lobe width is predicted by the diffraction of an opaque disk when the sphere size is greater than a couple of wavelengths (5,6) and, therefore, this lobe width is inversely proportional to the diameter of the sphere. Mullaney and Dean have shown (4) that the scattered intensity at an angle of 0.5° (which is within the central lobe) is approximately proportional to the volume of the sphere, and, therefore, a detector that measures this small-angle light scattering intensity will yield information about the volume distribution for a population of cells. However, as they have pointed out, the scattered intensity at this angle is a function of the index of refraction, and, therefore, one must assume that all the cells in the population have the same index of refraction. Also, as shown below, this scattered intensity at small angles is a function of the nucleus diameter to cell diameter ratio.

The simplest two-dimensional, two-parameter model that one could use to include some effects of the nucleus is to consider the diffraction from an opaque ring, as shown in Fig. 1. In this model, the outer edge of radius r_2 corresponds to the cellular size and the inner edge of radius r_1 corresponds to the nuclear size. This model essentially looks at only the diffraction effects of the edge of the cell and the edge of the nucleus.

Since the opaque ring is circularly symmetric, its scattering (or diffraction) pattern will also be circularly symmetric. The scattering pattern plot shown in Fig. 1 shows the angular dependence of the scattered light (where 0° corresponds to forward scattering). This scattering pattern is typical of the patterns of cells of different whole cell size ($\nu = 2\pi r_2/\lambda, \nu$ is called the whole cell size parameter) and nucleus to cell diameter ratio ($A = 2r_1/2r_2$). The central lobe width of this fine lobe structure shows the

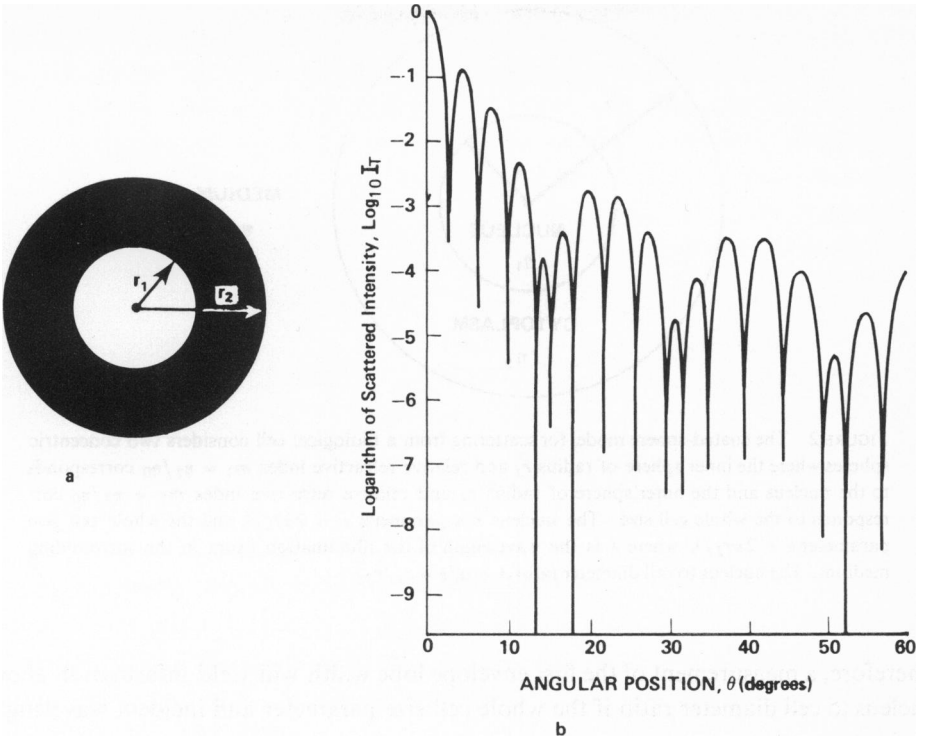

FIGURE 1 (*a*) The opaque ring scattering model is shown with a whole cell size parameter $\nu = 2\pi r_2/\lambda$, where λ is the wavelength of the illumination beam, and a nucleus to cell diameter ratio $A = r_1/r_2$. (*b*) A typical scattering pattern for an opaque ring with whole cell size parameter $\nu = 60$ and nucleus to cell diameter ratio $A = 0.6$. The logarithm of scattered intensity is shown as a function of angle where 0° corresponds to forward scattering.

well-known improved resolution (i.e., lobe narrowing) of an obstructed aperture (3). However, the sidelobes of this fine lobe structure are very similar in periodicity to the fine lobe structure of an opaque disk of equal size and illumination as the opaque ring, and therefore the fine lobe structure of the opaque ring scattering pattern is due mainly to the diffraction of the light at the outside boundaries of the cell. The envelope of the fine lobe structure (or low-frequency component of the pattern) in Fig. 1 is due to the interference between the light diffracted from the inner edge (nucleus) and the outer edge (whole cell). To summarize, then, the fine lobe structure contains information about the whole cell size and the envelope contains nucleus and cell size information.

Tschunko (7) has found that the number of fine lobe peaks between envelope minimums is independent of whole cell size and is inversely proportional to $(1 - A)$. The angular position, θ_{min}, of the first envelope minimum is given by

$$\begin{aligned} \sin(\theta_{min}) &= 2\pi\lambda/\nu(1 - A) \\ &= \lambda/(r_2 - r_1). \end{aligned} \tag{1}$$

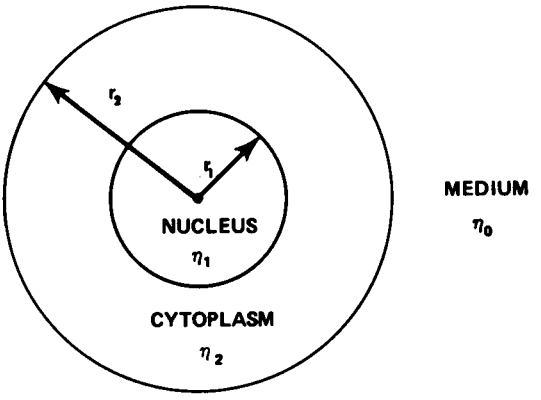

FIGURE 2 The coated-sphere model for scattering from a biological cell considers two concentric spheres where the inner sphere of radius r_1 and relative refractive index $m_1 = \eta_1/\eta_0$ corresponds to the nucleus and the outer sphere of radius r_2 and relative refractive index $m_2 = \eta_2/\eta_0$ corresponds to the whole cell size. The nucleus size parameter $\alpha = 2\pi r_1/\lambda$ and the whole cell size parameter $\nu = 2\pi r_2/\lambda$, where λ is the wavelength of the illumination beam in the surrounding medium. The nucleus to cell diameter ratio $A = \alpha/\nu = r_1/r_2$.

Therefore, a measurement of the first envelope lobe width will yield information about nucleus to cell diameter ratio if the whole cell size parameter and incident wavelength are known.

A coated sphere model (8–12) can be used to include the effects of nuclear and cellular diffraction, refraction, reflection, and absorption. This model considers two concentric spheres (see Fig. 2) of different index of refraction, where the inner sphere of radius r_1 corresponds to the nucleus of the cell and the outer sphere of radius r_2 corresponds to the cytoplasm. The scattering pattern for the coated sphere and the homogeneous sphere are shown in Fig. 3 (taken from ref. 9). The fine lobe structure for the homogeneous sphere and the coated sphere appear to be almost identical. The coated sphere scattering pattern also has an envelope lobe structure very similar to the diffraction pattern of the opaque ring as shown in Fig. 4. This was found to be true for almost all whole cell sizes and nucleus to cell diameter ratios considered, and suggests that the predominate mechanism in the scattering of a coated sphere at small angles is the diffraction at the edge of the nucleus and the edge of the cytoplasm. Apparently at larger angles, where the envelope structures of the coated sphere and the equivalent opaque ring differ, the effects of refraction and reflection become more important.

METHODS

Light scattering patterns for the coated and homogeneous spheres were computed as described previously (9). The light scattering pattern for the opaque ring (3) was computed by using the polynominal approximations of the first-order Bessel functions (13). Various comparisons between these models were then made as described below.

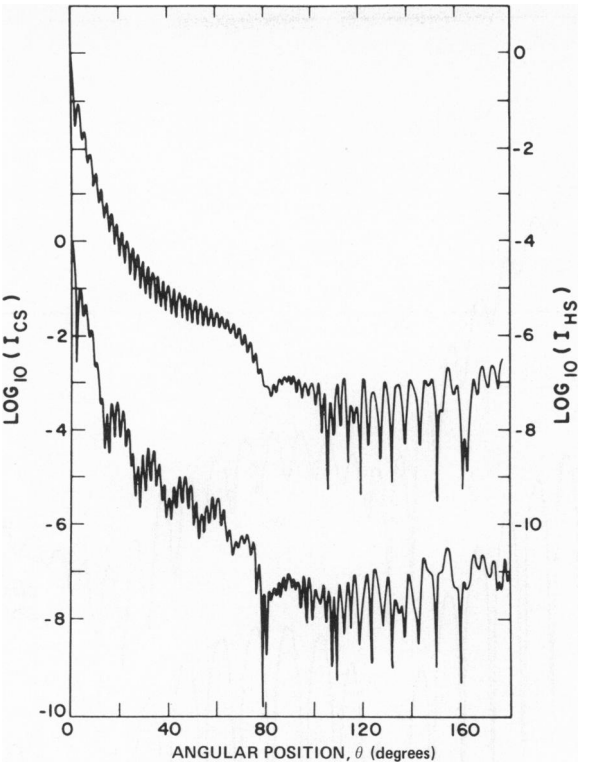

FIGURE 3 Logarithm of the relative intensity I vs. θ for a homogeneous sphere with $\alpha = \nu = 85$, $m_1 = 1.036$, $m_2 = 1.0$ (top curve), and a coated sphere with $\alpha = 2\nu/3 = 56.67$, $\nu = 85$, $m_1 = 1.05$, $m_2 = 1.03$ (bottom curve). I_{cs} and I_{HS} are the scattering intensities for the coated and homogeneous spheres, respectively. The plotting increment is 0.25° (taken from ref. 9).

RESULTS

Brunsting and Mullaney (9) have shown that the primary (i.e., high-frequency) central lobe width for the scattering pattern of a coated sphere is predicted by the diffraction of an opaque disk whose diameter is the same as the whole cell size for spheres with $\nu > 3$ (i.e., larger than a few wavelengths). This result was independent of nucleus to cell diameter ratio (A) over a limited range of refractive indices. The present technique for measuring this small-angle size information is to measure the intensity of the scattering pattern over a small angular region within the central lobe (2,4,14). The theoretical scattering intensity for a coated sphere measured by a single detector covering the angular region from 0° to 2° is shown in Fig. 5 as a function of whole cell size. This low-angle light scattering information is highly dependent on the nucleus to cell diameter ratio (A). To measure whole cell size independent of A, a different technique for measuring the central lobe width is required. One possible method would be to use two adjacent detectors located within the central lobe (15). The ratio of the output of these detectors would indicate the slope of the scattering intensity pattern and thus

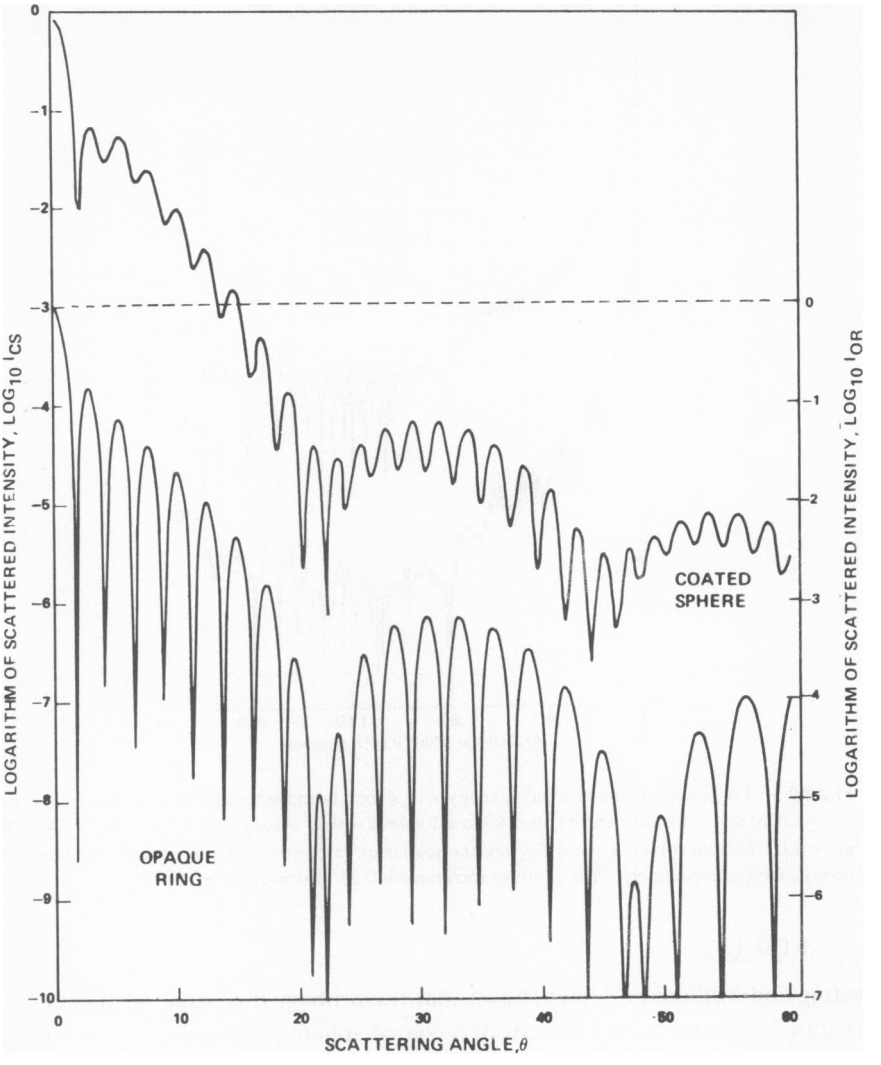

FIGURE 4 The logarithm of the relative intensity vs. angular position, θ, for a coated sphere (I_{cs}) and an opaque ring (I_{OR}) with $\nu = 85$, $A = 0.8$, and $m_1/m_2 = 1.05/1.03$. The plotting increment is 0.25°.

should indicate the central lobe width. In Fig. 6, the ratio of two 0.45° wide detectors centered at 1.5° and 0.5° is plotted as a function of whole cell size. For ν less than 50, this ratio is independent of nucleus to cell diameter ratio. For ν greater than 50, there is some dependence on A but not nearly as much as for the single-detector case (Fig. 5). In Fig. 7, the dependence of this signal on index of refraction ratio is indicated. The range of whole cell sizes over which this technique is sensitive can be

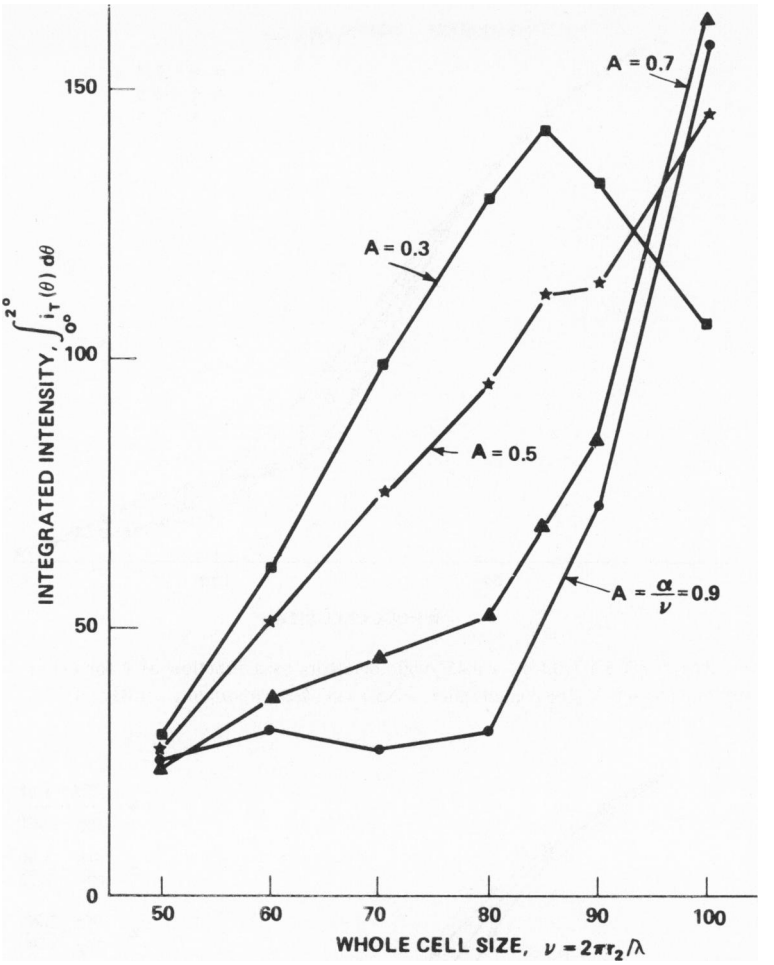

FIGURE 5 The low-angle scattering intensity for a coated sphere integrated over the region of $\theta = 0°$–$2°$ vs. whole cell size, ν, for different values of A and for $m_1/m_2 = 1.05/1.03$.

changed by using detectors located at different angles, as indicated in Fig. 8. These curves are very similar to those given by Mullaney and Dean (15) for the diffraction of an opaque disk, indicating that diffraction is the major mechanism determining the central lobe width for the coated sphere.

Since the envelope structure of the opaque ring scattering pattern provided information about the nucleus to cell diameter ratio (from eq. 1), the envelope structure of the coated sphere scattering pattern has been investigated in detail to determine if it also contains this information. The scattering patterns for three different coated spheres with the same whole cell size ($\nu = 85$) but with different nucleus to cell diameter ratios are shown in Fig. 9. A "filtering" technique has been used to suppress the fine

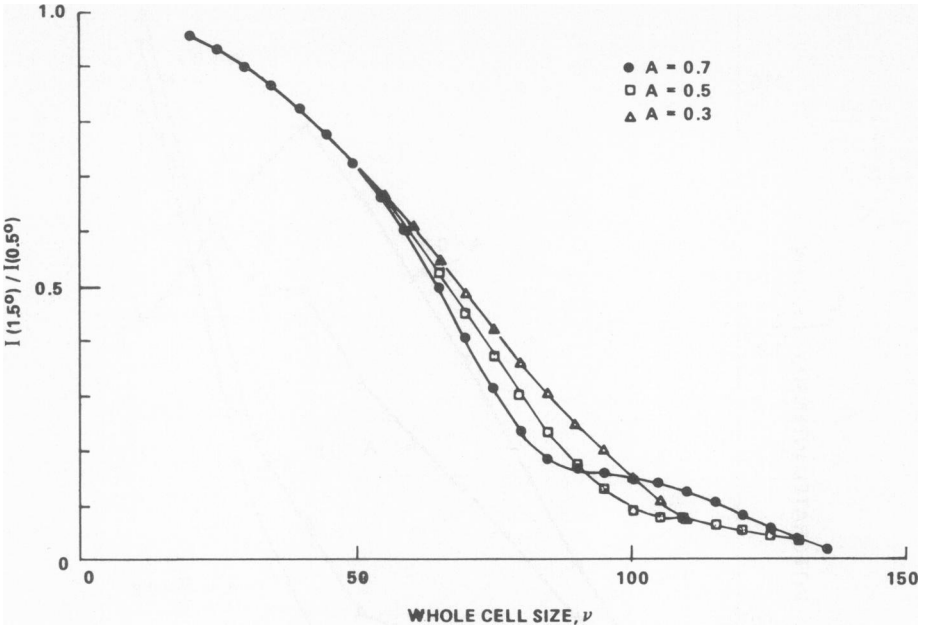

FIGURE 6 Plot of $I(1.5°)/I(0.5°)$ for 0.45° wide detectors as a function of ν for (·) $A = 0.7$, (□) $A = 0.5$, and (Δ) = 0.3. The coated sphere model was used with $m_1/m_2 = 1.05/1.03$.

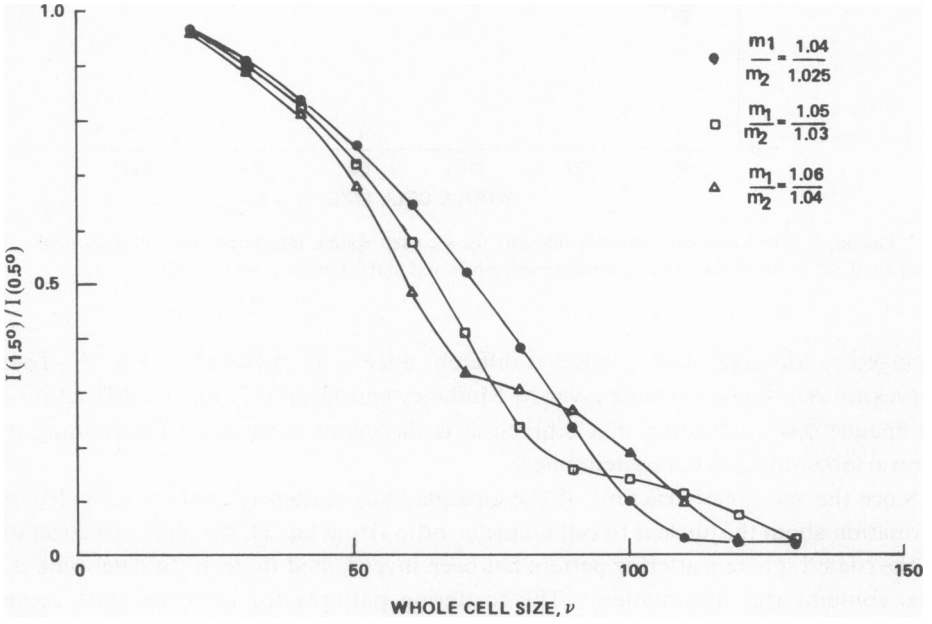

FIGURE 7 Plot of $I(1.5°)/I(0.5°)$ for 0.45° wide detectors as a function of ν for (·) $m_1/m_2 = 1.04/1.025$, (□) $m_1/m_2 = 1.05/1.03$, and (Δ) $m_1/m_2 = 1.06/1.04$. The coated sphere model was used with $A = 0.7$.

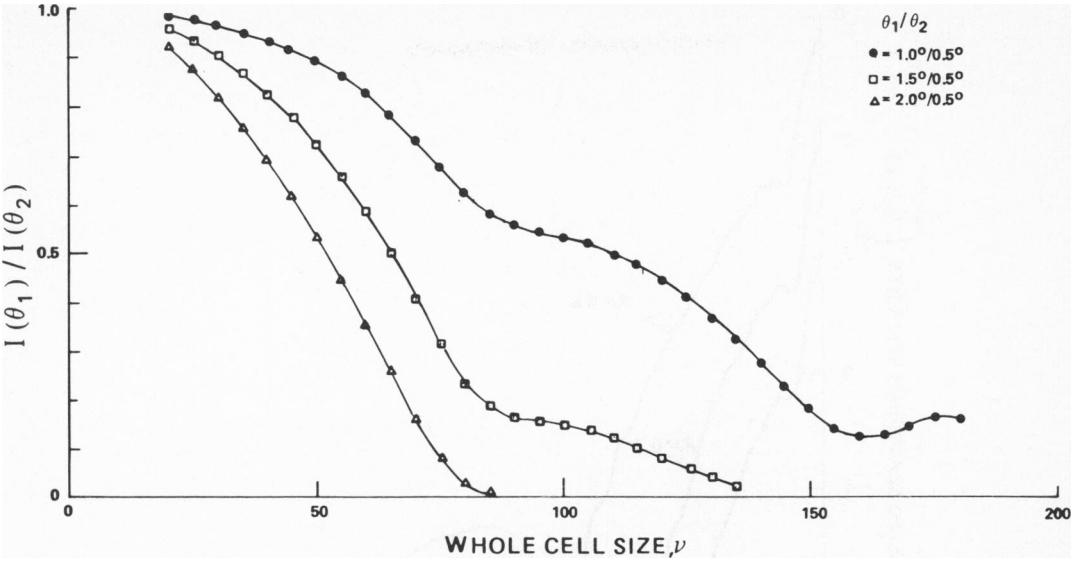

FIGURE 8 Plot of $I(\theta_1)/I(\theta_2)$ for 0.45° wide detectors for $\theta_2 = 0.5°$ and $(\cdot)\theta_1 = 1.0°$,$(\square)\theta_1 = 1.5°$, and $(\Delta)\theta_1 = 2.0°$. The coated sphere model was used with $A = 0.7$ and $m_1/m_2 = 1.05/1.03$.

lobe structure of the scattering patterns to see the envelope structure better. The scattering data was averaged over a 2° rectangular window and then this window was moved across the scattering pattern. Thus, the relative intensity at any point in the plots in Fig. 9 is approximately equivalent to the output of a 2° wide detector centered at that point. Three different values for nucleus to cell diameter ratio (A) are shown. As A decreases, the angular position of the first envelope minimum decreases as does the angular distance between maximums.

For some values of ν and A, it is difficult to locate the first envelope minimum; therefore, let us look at the average angular distance between maximums ($\overline{\Delta\theta}_{max}$). A plot of $1/\sin(\overline{\Delta\theta}_{max})$ as a function of nucleus to cell diameter ratio (A) for a constant whole cell size ($\nu = 85$) results in a straight line (Fig. 10). Straight lines also occur when $1/\sin(\overline{\Delta\theta}_{max})$ is plotted as a function of whole cell size for different nucleus to cell diameter ratios. The equation which describes these straight lines is

$$\sin(\overline{\Delta\theta}_{max}) \doteq 2\pi/\nu(1 - A) \doteq \lambda/(r_2 - r_1). \quad (2)$$

Notice that this equation is identical to eq. 1 for the opaque ring, which suggests that the major mechanism in the scattering by a coated sphere is the diffraction at the edge of the nucleus and the edge of the cytoplasm.

The average angular distance between envelope maximums ($\overline{\Delta\theta}_{max}$) was found to be independent of index of refraction ratio (m_1/m_2, where m_1 and m_2 are the relative index of refraction for the nucleus and cytoplasm, respectively). However, the angular

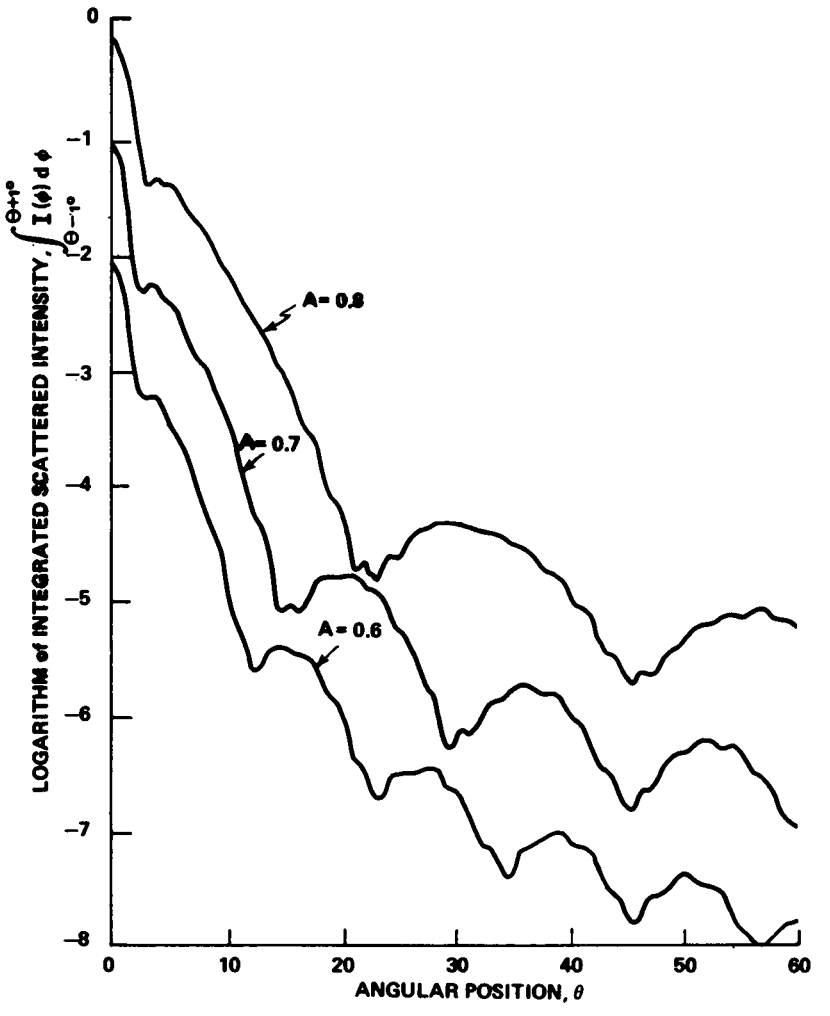

FIGURE 9 Logarithm of integrated scattered intensity, $\int_{\theta-1°}^{\theta+1°} I(\phi)d\phi$ as a function of θ for different values of A. The coated sphere model was used with $\nu = 85$ and $m_1/m_2 = 1.05/1.03$. The plotting increment is 0.25°.

position of the first envelope minimum is dependent on this index of refraction ratio. For the limited number of index of refraction ratios considered in this study (m_1/m_2 = 1.04/1.025, 1.05/1.03, and 1.06/1.04), we found that the angular position of the first envelope minimum increased by 10–20% as m_1 increased.

We have also noticed that the angular spacing of the envelope maximums are uniform on an I vs. θ plot for the coated sphere and on an I vs. sin θ plot for the opaque ring. One possible explanation for this is that as the angle, θ, between the detector and the incident light increases, the apparent size of the two-dimensional opaque ring as viewed by the detector decreases, whereas the apparent size for the

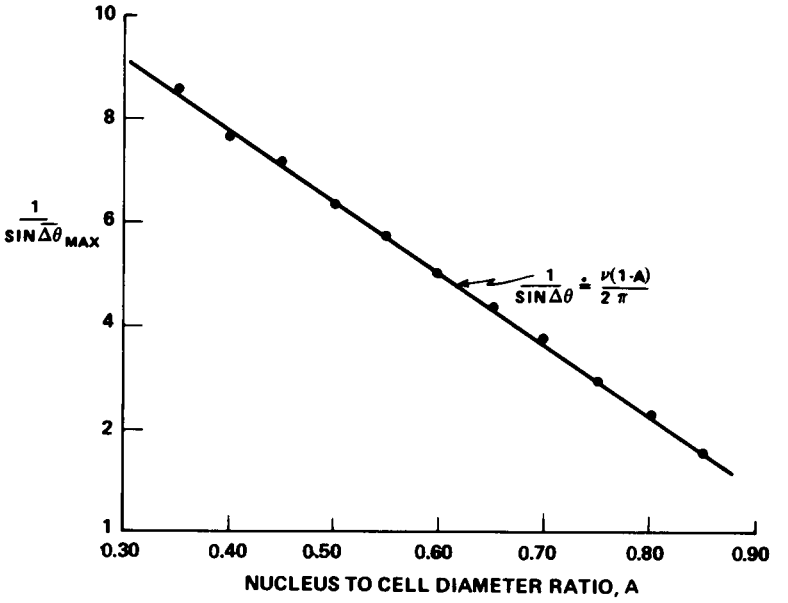

FIGURE 10 A plot of $1/\sin(\overline{\Delta\theta}_{max})$, where $\overline{\Delta\theta}_{max}$ is the angular distance between envelope maximums as a function of nucleus to cell diameter ratio, A. The coated sphere model was used with $\nu = 85$ and $m_1/m_2 = 1.06/1.04$.

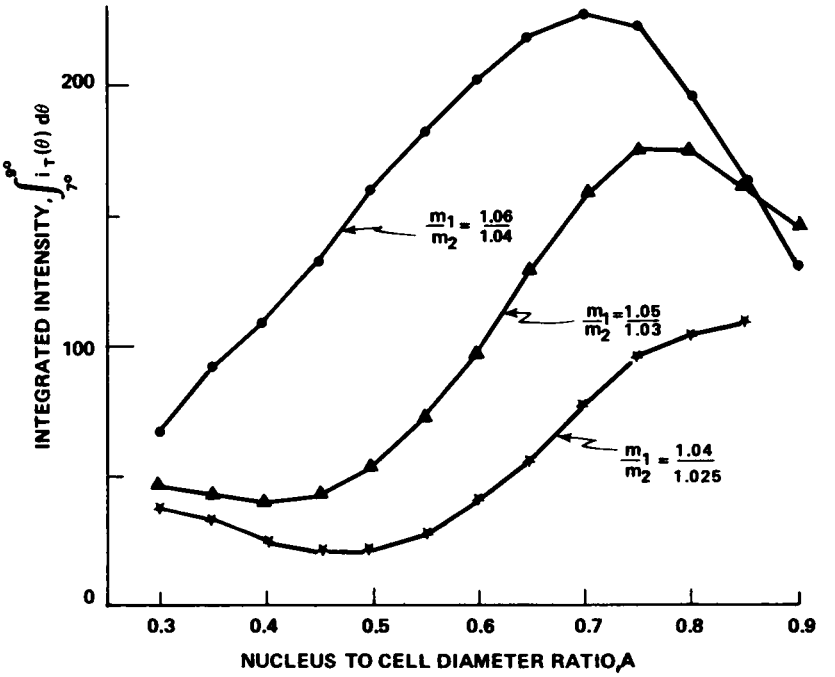

FIGURE 11 Scattered intensity integrated over $\theta = 7°$ to $\theta = 9°$ as a function of nucleus to cell diameter ratio A for (·) $m_1/m_2 = 1.06/1.04$, (▲) $m_1/m_2 = 1.05/1.03$, and (⋆) $m_1/m_2 = 1.04/1.025$. The coated-sphere model was used with $\nu = 85$.

three-dimensional coated sphere stays constant as θ increases. This difference in envelope maximum spacing could possibly allow one to discriminate between a flat and a rounded cell with the same size parameters.

Unfortunately, it is difficult to measure this angular distance between maximums. One would like to find an angular region in the scattering pattern where the output from a single detector element would yield information about the nucleus to cytoplasm ratio. We examined the output of a single detector located within the central lobe of the envelope pattern. The relative output from a detector covering the angular region from 7° to 9° is plotted in Fig. 11 as a function of nucleus to cell diameter ratio. If the relative index of refraction ratio is constant from cell to cell, the output from this detector gives a good measure of A over the region of $A = 0.4$–0.8. However, the result is heavily dependent on the relative index of refraction. In fact, if A were constant, this detector would probably result in a good measure of relative refractive index. Using the ratio of two detectors located within the first envelope lobe did not eliminate the dependence on the relative refractive index. A more detailed study is required to separate the effects of changes in nucleus to cell diameter ratio and relative refractive index.

CONCLUSIONS

Four theoretical models were used to approximate the scattered light from biological cells. By comparing the patterns of these models, the general physical processes for the scattering in the forward directions can be surmised. We have found that the major mechanism for the scattering at low angles is the diffraction of the light at the edge of the cell and the edge of the nucleus. We have suggested some techniques for experimentally extracting whole cell size and nucleus to cell diameter ratio.

Since the models consider an idealized cell, they ignore a number of physical parameters that will definitely affect the light scattering pattern (e.g., cells are not normally spherical, the nucleus is not usually centered within the cell, all cells have subcellular organelles). However, diffraction is still expected to play a dominate role in the scattering at low angles for these other cell types.

This work was supported by the National Institute of Neurological Diseases and Stroke under Grant NS 07226 (R. A. Meyer) and also by the Research Corporation (Dr. Brunsting). The authors also acknowledge the support of Auburn University and its computer center.

Received for publication 17 September 1974.

REFERENCES

1. BRUNSTING, A. 1974. Can light scattering techniques be applied to flow through cell analysis? *J. Histochem. Cytochem.* **22**:607.
2. MULLANEY, P. F., M. A. VAN DILLA, J. R. COULTER, and P. N. DEAN. 1969. Cell sizing: a light scattering photometer for rapid volume determination. *Rev. Sci. Instrum.* **40**:1029.
3. BORN, M., and E. WOLF. 1959. Principles of Optics. Pergamon Press, Inc., Elms Ford, N. Y.
4. MULLANEY, P. F., and P. N. DEAN. 1970. The small angle light scattering of biological cells. *Biophys. J.* **10**:764.

5. MULLANEY, P. F. 1970. Application of the Hodkinson scattering model to particles of low relative refractive index. *J. Opt. Soc. Am.* **60**:573.
6. KATTAWAR, G. W., and G. N. PLASS. 1967. Electromagnetic scattering from absorbing spheres. *Appl. Opt.* **6**:1377.
7. TSCHUNKO, H. F. A. 1974. Annular apertures with high obstruction. *Appl. Opt.* **13**:22.
8. ADEN, A. L., and M. KERKER. 1951. Scattering of electromagnetic waves from two concentric spheres. *J. Appl. Phys.* **22**:1242.
9. BRUNSTING, A., and P. F. MULLANEY. 1972. Light scattering from coated spheres: model for biological cells. *Appl. Opt.* **11**:675.
10. BRUNSTING, A., and P. F. MULLANEY. 1972. Differential light scattering: a possible method of mammalian cell identification. *J. Colloid Interface Sci.* **39**:492.
11. BRUNSTING, A., and P. F. MULLANEY. 1974. Differential light scattering from spherical mammalian cells. *Biophys. J.* **14**:439.
12. KERKER, M. 1969. The Scattering of Light. Academic Press, Inc., New York.
13. ABRAMOWITZ, M., and I. A. STEGUN, editors. 1964. In Handbook of Mathematical Functions. National Bureau of Standards, Washington, D. C.
14. STEINKAMP, J. A., M. J. FULWYLER, J. R. COULTER, R. D. HIEBERT, J. L. HORNEY, and P. F. MULLANEY. 1973. A new multiparameter separator for microscopic particles and biological cells. *Rev. Sci. Instrum.* **44**:1301.
15. MULLANEY, P. F., and P. N. DEAN. 1969. Cell sizing: A small-angle light scattering method for sizing particles of low refractive index. *Appl. Opt.* **8**:2361.